At-many-stations hydraulic-geometry for six major rivers originated from the Qinghai-Tibet Plateau

Chao Qin*[1], Baosheng Wu[1], Guangqian Wang[1], Ge Wang[1]
1 State Key Laboratory of Hydroscience and Engineering, Tsinghua University, PR China
*Corresponding Author, e-mail: glqinchao@nwsuaf.edu.cn

Abstract

At-many-stations hydraulic geometry (AMHG) has provided a novel way to understand river network development, simulate water flow and retrieve river discharge in data-scared regions. Based on in-situ measurements of six major rivers originating from the Qinghai-Tibet Plateau (QTP), this study verifies the existence of AMHG relations along the rivers and explores AMHG relations for cross sections that are not located in the same river reach. The mainstreams and tributaries of the studied rivers in the southern and the eastern portions of the QTP have satisfactory AMHG relation strengths with $R^2 > 0.9$ for over 60% of the relations. For cross sections located in the same stream order, approximately 60% (9/15) of the AMHG relations have an $R^2 > 0.6$. AMHG strength increases with increasing stream order; this finding reflects the increasing coherence and maturity of the river networks associated with the geomorphic shaping power of increased discharge. Width-AMHG intercepts are larger than those of depth- and velocity-AMHGs for all stream orders. Most of the generated from cross sections located in middle-scale rivers (orders 7-8) are within the observed range. Congruent hydraulics generally increase with an increase in in-situ measured hydraulics when the stream order increases. The AMHG relations existing among cross sections that are not located in the same reach, which is named as cross channel AMHG, indicate linear variability of cross-sectional geometric and hydraulic similarities in the same stream order. The results break the watershed divide boundary control on AMHG and have the potential to provide background knowledge for discharge estimation in mountain rivers located in the QTP.

Keywords: Cross channel AMHG, River networks, Stream order, Qinghai-Tibet Plateau, Yarlung Zangbo River; Lantsang River

1 Introduction

The power laws that hydraulic variables and flow discharges follow are referred to as hydraulic geometry (HG), and they describe the key role of river flow on river morphology (Leopold and Maddock, 1953). These geomorphic relationships were first discovered in the early 1910s by agricultural engineers in northern India and Pakistan to maintain fluvial equilibrium in constructed division channels. The HG theory was then constructed and proposed by Leopold and Maddock in 1953. HG has many notable practical utilities, including geomorphological assessment, routing and optimizing in hydrologic models, flood monitoring, water resource management, design of channel restoration, habitat studies for aquatic organisms and discharge estimates (Shields et al., 2003; Parker et al., 2007; Rosenfeld et al., 2007; Parker and Wilkerson, 2011; Neal et al., 2012; Bieger et al., 2015; Gleason et al., 2018; Kebede et al., 2020; Song et al., 2020). Theoretical research into the practical applications of HG has recently been a hotspot in river dynamics and fluvial geomorphology studies.

At-a-station hydraulic geometry (AHG) relates river width (w), water depth (d), flow velocity (v) and discharge (Q) over the range of discharges experienced at a cross section. Downstream hydraulic geometry (DHG) focuses on a reference discharge for a given flow recurrence frequency and the corresponding width, depth and velocity for cross sections that are downstream along a river. Overall, both the AHG and DHG follow the same empirical equation set:

$$w = aQ^b \quad (1)$$

$$d = cQ^f \quad (2)$$

$$v = kQ^m \quad (3)$$

where a, c and k are hydraulic geometry coefficients and b, f and m are hydraulic geometry exponents. The coefficients and the exponents are constrained by $ack = 1$ and $b+f+m = 1$, respectively, in the equation $Q = wdv$.

Hydraulic geometry and river morphology are interrelated by the frequency of flows and the stream order considering all cross sections in a catchment boundary (Stall and Fok, 1968). Followers tried to explore basin wide hydraulic geometry in account of the idea that "cross sections of a given stream system are interrelated" (Stall and Yang, 1970; Rhodes, 1977). Basin hydraulic geometry, defines the average values of w, d, and v for a given streamflow or for a given flow duration and drainage area, reveals general characters of a given stream network in a hydrologically homogeneous basin (Singh and Broeren, 1989). Following this chain, Gleason and Smith (2014) proposed AMHG, a geomorphic phenomenon that spatially and temporally links river cross sections along a river reach (AHG coefficients and exponents statistically relating w, d, and v to Q). Linear correlations were found between AHG exponents (b, f, m) and log (AHG coefficients) (a, c, k) (e.g., $b = \alpha \log a + \beta$, $f = \gamma \log c + \mu$, and $m = x \log k +$

η). Therefore, the AMHG for a user-defined length of a river is defined as follows (Gleason and Smith, 2014):

$$w_c = a_{x1,x2,\ldots,xn} Q_{cw}{}^{b_{x1,\,x2,\ldots,xn}} \quad (4)$$

$$d_c = c_{x1,x2,\ldots,xn} Q_{cd}{}^{f_{x1,\,x2,\ldots,xn}} \quad (5)$$

$$v_c = k_{x1,x2,\ldots,xn} Q_{cv}{}^{m_{x1,\,x2,\ldots,xn}} \quad (6)$$

where subscript *c* refers to "congruent hydraulics", the empirically fit river-specific constants that define AMHG, *a*/*c*/*k* and *b*/*f*/*m* are site-specific AHG coefficients and exponents in Eq. (1)-(3) at each cross section, and subscripts *x*1, *x*2, … *x*n correspond to spatially indexed cross-section locations (up to *n* total cross-sections along a river reach).

Although not universally observed on natural rivers, AMHG is frequently verified and comprehensively reflects the relationship between the coefficients and exponents of AHG (Gleason et al., 2018). Some studies sought to verify the empirical relations across a wide range of physiographic settings, while other studies aimed to discover the theoretical basis of AMHG and apply this theory to discharge estimation. In summary, three key subjects related to AMHG research and can be summarized as follows: 1) the existence of AMHG as a geomorphological phenomenon for river reaches across various environments with differing climates, geologies, geomorphologies, soil, among others (Gleason and Wang, 2015; Shen et al., 2016; Barber and Gleason, 2018); 2) the theoretical basis for AMHG, including the calculation and proof of congruent hydraulics (Gleason and Wang, 2015; Barber and Gleason, 2018; Brinkerhoff et al., 2019); and 3) the development of river discharge and sediment estimates based on AMHG and further development of Bayesian AMHG-Manning (BAM) with and without prior in-situ measurements (Gleason et al., 2014; Gleason and Hamdan, 2017; Hagemann et al., 2017; Gleason et al., 2018; Zhao et al., 2019; Brinkerhoff et al., 2020; Flores et al., 2020).

As a geomorphic index, congruent hydraulics depict shared characteristics within a certain range of settings. AMHG suggests that there are a set of width-, depth- and velocity-discharge values that are shared by all cross sections within a river (Gleason, 2015). How to depict the mutual characteristics that are shared between individual cross sections has attracted much attention. Gleason and Smith (2014) found that the relationship between Ln (*AHG coefficients*) and *AHG exponents* of any pair of cross sections in a river reach is linear with a slope equivalent to:

$$\text{AMHG } slope = \frac{b_{x2} - b_{x1}}{\text{Ln}\,(a_{x2} - a_{x1})} \quad (7)$$

Exponent *b* and coefficient *a* can be replaced with exponents *f*, *m* and coefficients *c*, *k*, respectively. Eq. (7) affirms that there should be theoretical *w*~*Q*, *d*~*Q* and *v*~*Q* pairs that are shared by all cross sections along a river reach. Gleason and Wang (2015) studied the mathematical basis and geomorphological implications of AMHG. They discovered that AMHG arises from the convergence of rating curves and can be represented by congruent hydraulic pairs (w_c~Q_c, d_c~Q_c, v_c~Q_c), which are temporally and spatially invariable (Barber and Gleason, 2018). However, the existence of congruent hydraulics and their relationships to AMHG have not been thoroughly examined and are not well understood though a series of follow-up researches were conducted (Brinkerhoff et al., 2019). Barber and Gleason (2018) sought to establish correlations between common fluvial parameters and indices to investigate potential driving factors of AMHG for rivers with a strong AMHG presence, and they used 191 rivers in the US to perform this test. However, no correlation between AMHG strength and congruent hydraulics, or average values of in-situ measured discharge, width, depth, and velocity, has been discovered (Barber and Gleason, 2018). Brinkerhoff et al. (2019) investigated the relationships between AMHG strength and local features (cross section morphology, bed slope and boundary roughness) of individual cross sections. They found that a strong AMHG is a result of a strong slope/resistance relationship between the stations used to define AMHG. Congruent hydraulics can either be within or outside the in-situ measured range (Gleason and Wang, 2015). In Barber and Gleason's (2018) research, 118 of the 191 rivers show a strong AMHG with $R^2 > 0.6$. Specifically, over 77% of rivers with strong AMHG and only 30% of rivers with weak AMHG had a Q_c value that fell within the range of observed discharges.

More than 80% of the published papers regarding AMHG are focused on or related to the retrieval of river discharge and sediment data, relying on the applications of remote sensing or photogrammetry. AMHG allows reach-averaged discharge to be estimated where cross-sectional widths can be extracted from satellite data. Gleason et al. (2014) proposed an AMHG-based remote sensing discharge retrieval algorithm, which works for mass-conserved reaches and produced errors within 20%-30% of in-situ measured discharge in different types of rivers. Hagemann et al. (2017) developed the AMHG theory into BAM, which estimates river discharge using physical/empirical flow-law (Manning's equation) and geometric/empirical flow law (AMHG) in a probabilistic manner. Feng et al. (2019) affirmed the possibility of estimating discharge independent of ground-based measurements with BAM. Recently, geo-BAM method proposed by Brinkerhoff et al. (2020) and decile thresholding discharge estimation method developed by Mengen et al. (2020) contribute to a significant improvement in discharge estimation. However, estimation accuracy of the aforementioned method using only satellite-observed cross-sectional width data is not always guaranteed if no previous estimates were made (Hagemann et al., 2017; Brinkerhoff et al, 2020). The availability of gauge data and the accurate estimation of the AMHG can significantly improve the performance of

discharge estimations (Bonnema et al., 2016).

As seen from the previous research regarding AMHG, less consideration has been taken into account for those cross sections across river reaches, although parameters across sites were linked and spatial relationships of cross-sectional morphologies were reflected in terms of the same river reach (Shen et al., 2016). This research gap prohibits a deeper understanding of river network distribution as well as the development and application of water flow simulations and estimates of river discharge in a broader scope. As the flowing water and sediment shape the river morphology to some extent, can we expect morphologies of cross sections across river reaches to be linked if they experience a similar stream order? Does AMHG exist across rivers, regions, or other configurations? Therefore, it is necessary to expand the AMHG scope (e.g. across river reaches) to facilitate research on geomorphological assessment, routing and optimizing in hydrologic models, flood monitoring and water resource management, among others.

The Qinghai-Tibet Plateau (QTP), known as Asia's Water Tower, is the origin of ten major rivers flowing through the Asian continent. This region covers a wide range of climates and underlying surface characteristics, including differing geologies, geomorphologies, and soil and vegetation types. Rivers of different stream orders show a wide variety of stream patterns from single-thread to multi-thread and from rock-constrained to free-flow. Whether the rivers in the QTP conform to the AMHG theory or if any spatial distribution can be found for AMHG relations in this region are inquiries that need to be addressed. Width, depth and velocity AMHG has been examined, with studies that have been mainly concentrated on US rivers encompassing a wide range of climate and geologic settings (Gleason and Smith, 2014; Shen et al., 2016; Barber and Gleason, 2018). Weak AMHG relations were mostly concentrated in the area of the western edge of the Rocky Mountains, while a total of five and eleven rivers along the northwest and southeast coasts, respectively, were identified as having statistically strong AMHG (Barber and Gleason, 2018). However, the weak AMHG relations of Rocky Mountains are based on limited dataset, which is worth to be further verified in other mountainous regions (Barber and Gleason, 2018). For mountain rivers located in the QTP, AMHG research is nearly nonexistent according to our literature review. The existence and spatial distribution of AMHG, which has not been confirmed but is thought to be influenced by climate and geomorphology, can be further explored in the complex environments present in the QTP (Barber and Gleason, 2018).

In summary, following are some research gaps regarding AMHG theory and application: (a) AMHG knowledge based on in-situ measurements is very limited for data-scared mountain rivers, which contributes less to understanding of river network distribution and development, and results in low accuracy of discharge estimation in these regions (Hagemann et al., 2017); (b) whether it is necessary to confine the AMHG relations to a given river reach might be questioned; (c) except for slope and flow resistance, how would the spatial features (stream order) affect AMHG strength and congruent hydraulics. Due to the limitations of previous research, this article aims to (1) verify the existence of AMHG relations for mountain rivers located in the southern and the eastern portions of the QTP; (2) explore spatial distributions of AMHG exists for cross sections across river reaches; and (3) discuss the relationships between congruent hydraulics and stream order as well as in-situ measured hydraulics.

2 Data and Methods

2.1 Studied area

The studied region, which includes basins of the upper Yellow River (YR), the Yalong River (YLR), the upper Jinsha River (JSR), the Lantsang River (LCR), the Nu River (NR) and the Yarlung Zangbo River (YLZBR), is mainly located in the southern and the eastern portions of the QTP, which is within the Qinghai, Sichuan, Gansu, and Yunnan provinces and the Tibet Autonomous Region of China (Fig. 1). The total area of the studied region is 130.787×10^4 km^2. To maintain the integrity of the upper Yellow River, portions of the connecting regions between the QTP and the Loess Plateau are included. Similarly, marginal regions that belong to the upper Jinsha River, the Lantsang River and the Nu River are also included in this study, though they are outside the southern and eastern portions of the QTP (Fig. 1). The landscape of the studied region, especially for transient regions, is highly fragmented and heavily influenced by tectonic movement and geological disasters (Qin et al., 2020). Hillslope-channel coupling (high potential of hillslope sediment delivery to streams) affects channel forms in mountainous regions (Hassan et al., 2019). But the studied cross sections of our research are mainly located in straight reaches where rarely suffered from landslides, debris flows, glacial outbursts and other extreme events. The elevation shows a decreasing trend from > 7300 m in the inland QTP to < 150 m in the southernmost area. The annual precipitation increases from 150 mm in the inland QTP to > 4000 mm near the town on Pasighat in the Yarlung Zangbo River (Ding et al., 2007). The main discharge sources include the melting of the persistent winter snowpack, glacial deposits acting as groundwater reservoirs of the inland QTP and summer rainstorms in the remaining area.

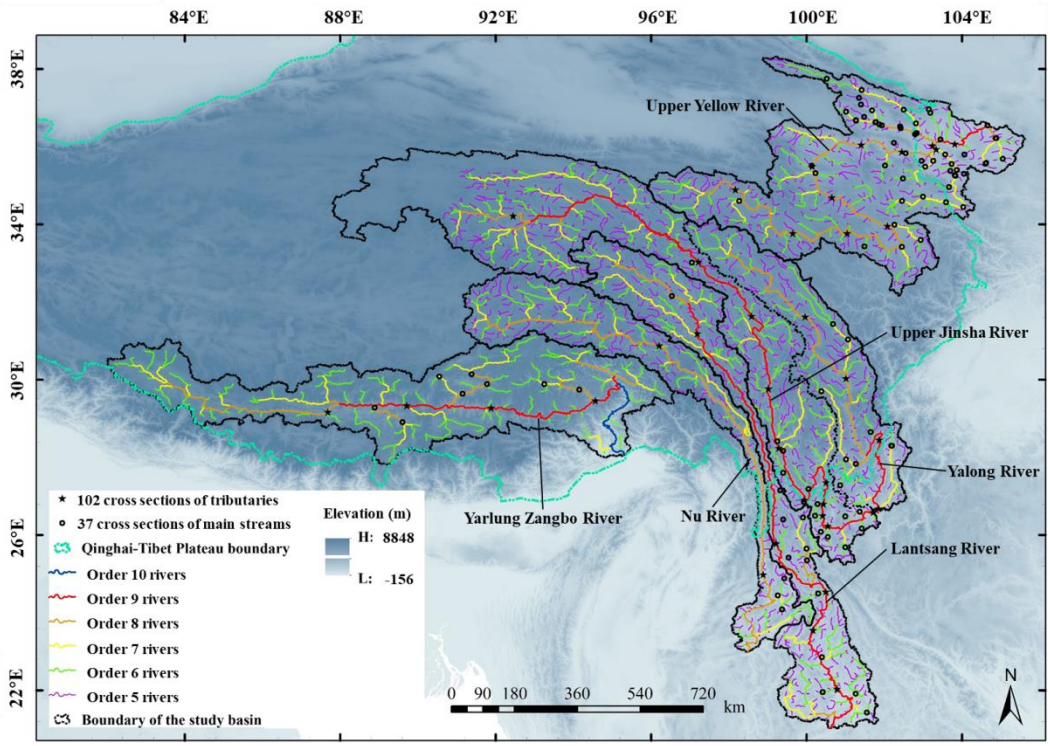

Figure 1 Location of the studied region

2.2 Data collection

The data used in this study were acquired from Annual Hydrological Reports of P. R. China (1967-2017). The measurements of flow characteristics (river width, water depth, flow velocity and flow discharge) and cross-section morphology were conducted strictly in accordance with the national standard of China, "Code for water flow measurement in open channels" (Ministry of Water Resources, P. R. China, 2016). The data set have certain representativeness of mountain rivers. Contributing area, river width, flow depth, flow velocity and flow discharge were within the ranges of 83-259177 km^2, 1.4-420 m, 0.08-21.2 m, 0.05-5.02 m s^{-1} and 0.03-10400 m^3 s^{-1}, respectively. The dataset consisted of 139 river cross sections and covered a wide range of stream patterns from single-thread (represented by straight and meandering rivers) to multi-thread (represented by braided rivers).

The SRTM 90 m DEM (can be downloaded from "http://www.gscloud.cn/") and ArcGIS 10.5 (ESRI Inc., Redlands, CA, USA) were used to generate river networks. Threshold filtering method was used to generate river networks (Mark, 1984; Martz and Garbrecht, 1992). We set a flow accumulation threshold of 40 (equals to 0.324 km^2) after trial-and-error and found that the generated river networks matched the rivers presented in Google Earth images well. The stream orders of the studied region were 1st through 10th, and only the cross sections located in order 5-9 streams were presented in this study because the available measurements were mainly concentrated in rivers of these orders (Fig. 1 and Table 1).

Table 1 Numbers of cross sections at different stream orders

River system	5	6	7	8	9	Total
Upper Yellow River	14	21	17	14	1	67
Yalong River	0	5	4	3	1	13
Upper Jinsha River	0	11	2	2	10	25
Lantsang River	3	5	2	2	5	17
Nu River	1	1	1	2	0	5
Yarlung Zangbo River	0	0	2	7	3	12
Total	18	43	28	30	20	139

2.3 Data Processing

2.3.1 Criteria for data screening

A total of 201 measured river cross sections (obtained from national and regional hydrological gauge stations) are located in the studied area, and 139 of them were selected for analysis in this study. Percentages of the selected cross sections to the total cross sections are 71%, 76%, 74%, 74%, 56% and 50% for the upper Yellow River, the Yalong River, the upper Jinsha River, the Lantsang River, the Nu River and the Yarlung Zangbo River, respectively (Table 1). The criteria for the filtering of river cross sections were as follows: the cross sections should 1) have a consecutive hydrological record length exceeding 10 years; 2) have had relatively low anthropogenic influence (e.g., no hydropower station and artificial diversion 10 km upstream and downstream of the measured cross section; located outside the backwater zone of a dam) during the study time period to maximum remove the external disturbance; 3) keep away from the region where might be affected by extreme events like glacial outbursts, landslides et al.; and 4) act as a natural riverway with perineal drainage. After initial filtering based on these four criteria, cross sections were then re-filtered based on their AHG strength, evaluated by $R^2 > 0.6$ of the power regression for $w/d/v \sim Q$ relations to generate reliable and representative AMHG relations and avoid possible bias of data limitations. Due to the significant effects of ice on AHG relations (Qin et al., 2020), data that were affected by border ice, slush ice run and ice cover were excluded. Finally, unrealistic fittings (cross sections with fitted AHG exponents (b, f or m) that were < 0) were removed.

2.3.2 Calculation of the AMHG

Power functions depicting the relationships of $Q \sim w$, $Q \sim h$ and $Q \sim v$ were first fitted using the least squares method in MATLAB 2018b. The AHG coefficients, exponents and R^2 of the fittings were recorded. A minimum number of 4 cross sections was used to calculate the AMHG relations in this study. Considering the whole studied region, the AMHG fitted by 4 cross sections (Yalong River, Yarlung Zangbo River) can be regarded as a reference in analyzing spatial distributions when the AMHG relation is strong. Additionally, Barber and Gleason (2018) indicated that no correlation was found between the number of cross sections (> 6) used to calculate AMHG and the AMHG strength. Finally, the AMHG of five main streams (excluding Nu River as there were only 2 measured cross sections) and one secondary tributary of the Yellow River (Datong River) were fitted (Fig. 2). The lengths of these six reaches range from 370 to 2744 km, which are longer than those used for discharge retrievals based on remote sensing images (Feng et al., 2019). Mass was not conserved, and discharge increased downstream with the confluence of tributaries.

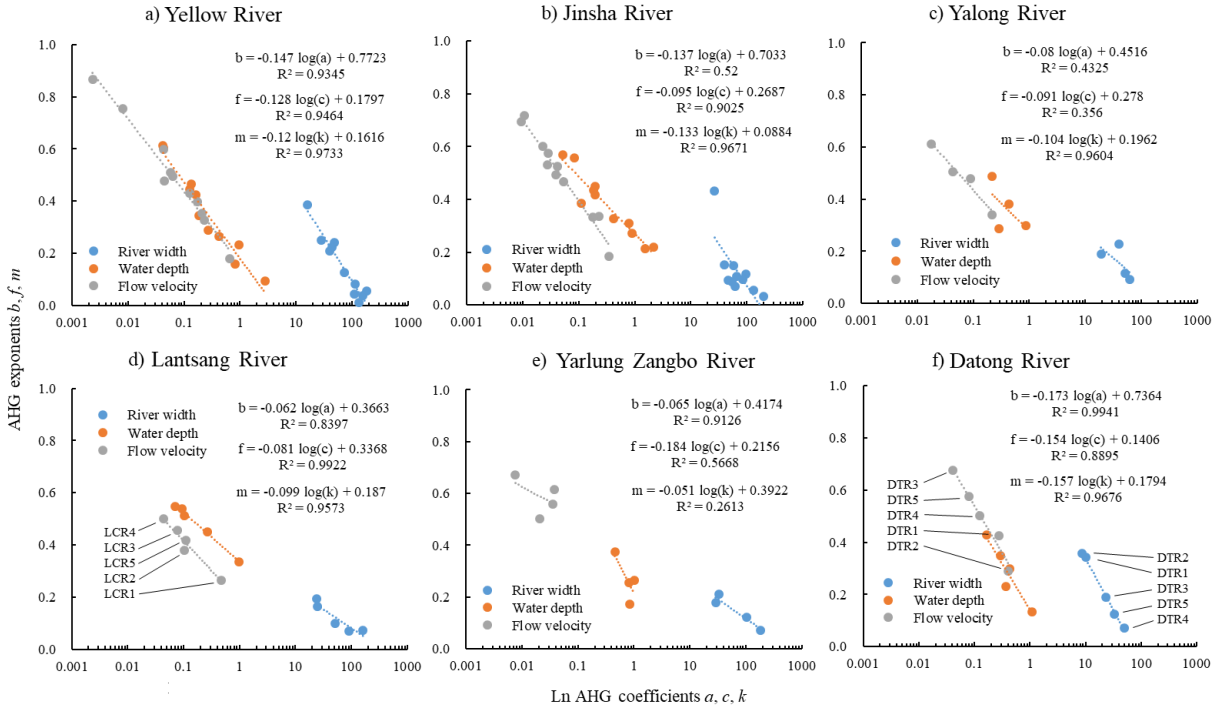

Figure 2 AMHG of five main streams (a-e) and one tributary of the Yellow River (f)

To explore AMHG relations across river reaches, five stream orders (orders 5-9) were considered in account of different clustering modes of cross sections. The following is the AMHG relations of different stream orders (revised from Gleason and Smith, 2014):

$$w_c = a_{x1,x2,\ldots,xn} Q_{cw_{O_i}}^{b_{x1,x2,\ldots,xn}} \quad (8)$$

where the subscripts $x1, x2, \ldots xn$ correspond to spatially indexed cross-section locations (up to n total cross sections at each stream order), O_i represents the stream order i (i = 5, 6, 7, 8, 9). Similarly, depth-AMHG and velocity-AMHG can be formulated in the same way. Cross channel AMHG, generated from cross sections that are located across river reaches but in the same stream order (Eq. 8), is defined to reflect the hydraulic self-similarity of cross sections and the consistency of AHG coefficients and exponents across reaches.

Gleason and Wang (2015) proposed that the linearity (R^2) of AMHG should be interpreted as a geomorphic index indicating the degree of convergence of AHG curves, the cross-sectional geometric variability, and the hydraulic self-similarity of a given river reach. Therefore, the strength of the AMHG can be represented by R^2 of the fitted AMHG curve. Congruent hydraulic pairs (Q_{cw}, w_c; Q_{cd}, d_c; Q_{cv}, v_c) represent the intersections of the AHG rating curves (Gleason and Wang, 2015). For rivers that exhibit strong AMHG, Q_{cw}, Q_{cd}, Q_{cv}, w_c, d_c, and v_c are given by the spatial mode of the time mean of each of these cross-sectional quantities (Gleason and Wang, 2015). To reach the minimum divergence of the rating curves, two conditions to be met: 1) sufficient variability of the AHG exponents and 2) AMHG where $R^2 > 0.5$ (congruent hydraulics without superscript [b] in Table 2).

Table 2 Congruent hydraulics and their corresponding mean hydraulics clustered by river reaches and stream orders (of six river reaches and those in the same stream order)

Items	Log (Q_{c_w})[a]	Log (Q_{c_d})[a]	Log (Q_{c_v})[a]	Log (w_c)[a]	Log (d_c)[a]	Log (v_c)[a]	Mean Q	Mean w	Mean d	Mean v
Upper Yellow River	6.8	7.8	8.3	5.3	1.4	1.3	725.4	161.9	2.66	1.50
Upper Jinsha River	7.3	10.5[c]	7.5	5.1	2.8	0.7	2029.0	165.3	5.81	1.89
Yalong River	12.5[bc]	11.0[bc]	9.6[c]	5.6[bc]	3.1[bc]	1.9[c]	1619.2	115.6	5.97	1.88
Lantsang River	16.1[c]	12.3[c]	10.1[c]	5.9[c]	4.2[c]	1.9[c]	1857.3	140.5	6.41	2.10
Yarlung Zangbo River	15.4[c]	5.4	19.6[bc]	6.4[c]	1.2	7.7[bc]	1815.3	196.6	5.83	1.24
Datong River	5.8	6.5	6.4	4.3	0.9	1.1	172.6	54.9	1.53	1.54
Order 5 rivers	8.6[bc]	7.5[bc]	11.8[bc]	3.9[bc]	1.3[bc]	4.4[b]	10.1	13.7	0.40	0.94
Order 6 rivers	7.3[b]	8.2[c]	8.2[c]	4.1[b]	1.6[c]	2.4[c]	47.1	28.9	0.86	1.08
Order 7 rivers	8.0	6.4	7.8	4.7	0.9	1.7[c]	139.2	62.8	1.25	1.26
Order 8 rivers	9.4[c]	7.8	8.8	5.3	1.5	1.8[c]	561.7	115.2	2.51	1.45
Order 9 rivers	17.9[c]	9.2[c]	9.8	6.1[c]	1.5	2.7[c]	2139.0	166.1	6.41	1.92

[a] represents natural log, [b] represents the R^2 of the fitted AMHG is smaller than 0.5, and [c] represents the congruent value does not occur within the range of observed values.

3 Results

3.1 AMHG of the cross sections in a given river reach

Data from the six reaches, which include five main streams and one tributary of the Yellow River, were used to explore the relationships between AHG coefficients and exponents along a river reach. In terms of three AMHG relations (width-, depth- and velocity-) for all reaches, there is at least one relation for each reach that has an $R^2 > 0.9$ (Fig. 2). For the four reaches (Yellow River, Jinsha River, Lantsang River, Datong River) that have > 5 in-situ measured cross sections, the R^2 of the fitted AMHG relations are > 0.8, excluding the width-AMHG of the Jinsha River (Fig. 2 a, b, d, f). The outlier of the width-AMHG of the Jinsha River (shown as a blue circle in Fig. 2 b) corresponds to the Tuotuo River cross section, which is located in a braided reach, while all other cross sections of the Jinsha River (JSR2 to JSR11, Qin et al., 2020) are located in single thread reaches. Stream pattern might be a factor that influence the AMHG relation. However, due to very few cross sections are located in braided reaches, we are unable to generate AMHG relations of braided rivers alone. Cross sections located in all stream patterns are combined in the analysis. Our future work will focus on the classification of stream patterns with the help of remote sensing imagery interpretation. Then, cross sections will be clustered by single-thread and multi-thread river reaches to generate AMHG relations.

Additionally, the R^2 of the width-AMHG is usually smaller than those of the depth- and velocity-AMHGs (Fig. 2). These results agree with previous studies conducted by Gleason and Smith (2014), Gleason and Wang (2015), and Shen et al. (2016). This finding is likely due to the fact that river width is more sensitive to the variations of discharges

and boundary conditions than water depth and flow velocity. Random variations of river width are evident while water depth and flow velocity show relatively stable status. Less consistent variations of river widths leads to a weaker strength of width-AMHG.

The relative relations between the depth-AMHG and the velocity-AMHG differ between the Yellow River (including its tributary) and other rivers. The curves of the depth-AMHG and the velocity-AMHG for the Yellow River and Datong River nearly overlap as shown in Fig. 2 a and f. The two curves have similar slopes and intercepts. However, the curves of the depth-AMHG for the remaining river reaches (excluding the Yarlung Zangbo River) are located to the upper right of the velocity-AMHG curves. In conclusion, AHG coefficients and exponents in the same river reach show high correlation on a spatial scale under the original definition for AMHG in the southern and eastern portions of the QTP. Both our study and Barber and Gleason's research (Barber and Gleason 2018) have focused on mountain regions. Strong AMHGs were verified in the QTP region (AMHG strength $R^2 > 0.8$, Fig. 2) while relatively weak AMHGs were observed in the Rocky Mountain area (AMHG strength $R^2 < 0.4$). One possible explanation might be attributed to that the rivers located in west Rocky Mountains own lower stream orders than those of the rivers located in the QTP. Of course, more information of local climate, geology, geomorphology, soil and vegetation et al. are needed for further comprehensive explanations.

3.2 AMHG of the cross sections in the same stream order

3.2.1 AMHG for cross sections of individual river basins

AMHG relations are fitted at different stream orders to explore the existence of AMHG for individual river basins and study the spatial distribution of the AMHGs. The Yalong River is the largest tributary of the upper Jinsha River and merges into the upper Jinsha River in Panzhihua City (26.61°N, 101.81°E) (Fig. 1). Therefore, these two rivers are combined and analyzed in Section 3.2.1 (Fig. 3).

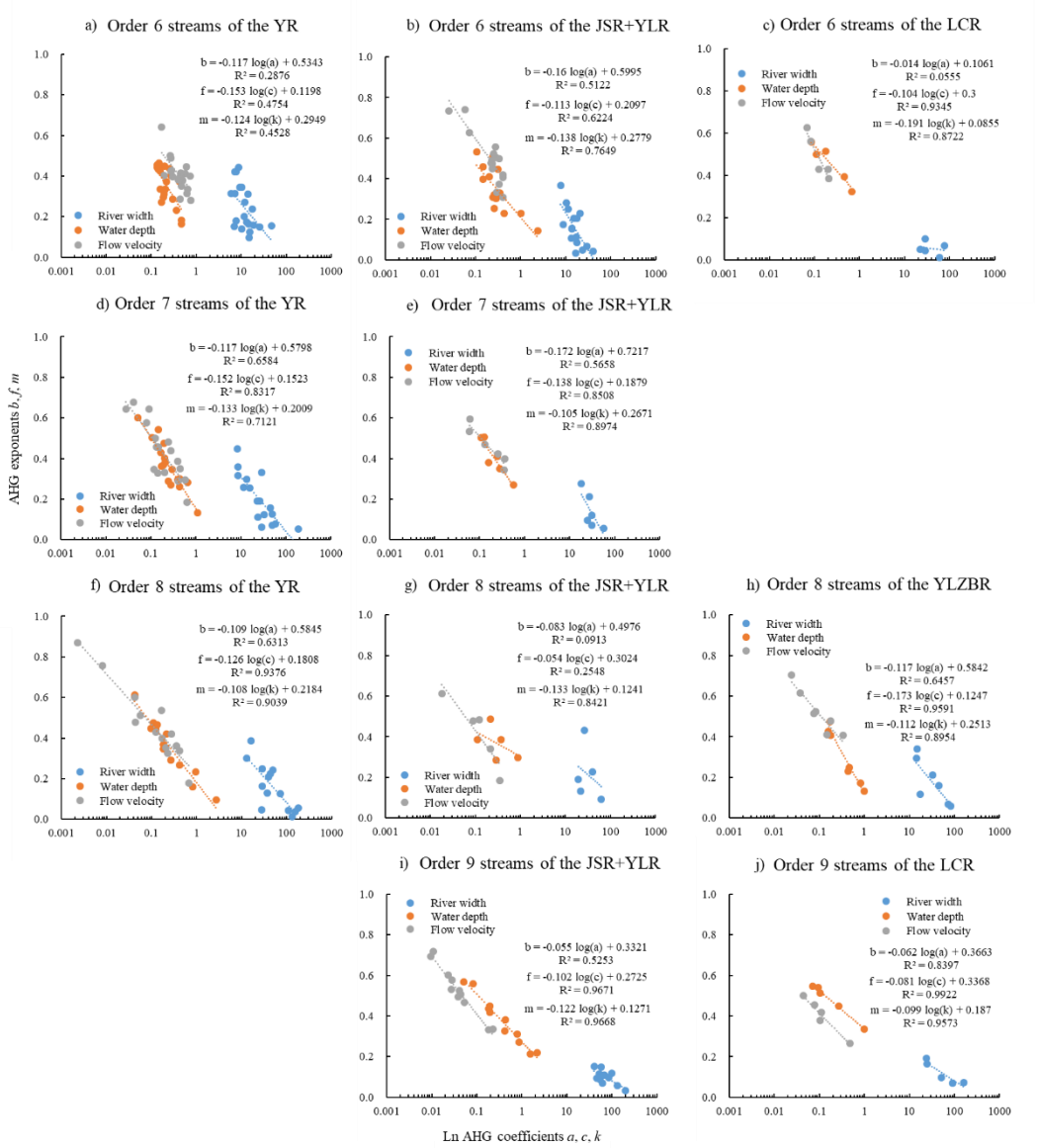

Figure 3 AMHG for cross sections located in the Upper Yellow River Basin, the Upper Jinsha River + Yalong River Basin, the Lantsang River Basin, the Yarlung Zangbo River Basin at stream orders 6 (a-c), 7 (d, e), 8 (f-h) and 9 (i, j).

When considering the same river basin but different stream orders, the strengths of the three AMHG relations for individual river basins generally increase with increasing stream order, excluding order 8 streams of the Jinsha River + Yalong River, as shown in Fig. 3 g. When considering the same stream order but different river basins, the AMHG exhibits varied spatial distribution. The Yellow River, Jinsha River + Yalong River, and Lantsang River are located from north to south in the eastern part of the QTP. Absolute values for depth-AMHG slopes for these river basins decrease from north to south within the same stream order (Fig. 3). This pattern is potentially because the mean annual discharge generally increases from north to south, which is determined by the local climate and landscape. This result also verifies the increasing trend of Q_{c_w} for all studied reaches from north to south of the eastern QTP (Table 2). Additionally, when compared with the AMHG strength of the mainstream of the Yarlung Zangbo River, the AMHG strength of the cross sections located in order 8 streams of the Yarlung Zangbo River Basin exhibit stronger correlations (Fig. 2 e and Fig. 3 h). Specifically, the depth- and velocity-AMHG strengths of the order 8 streams of the Yarlung Zangbo River Basin are much stronger than those of the mainstream of the Yarlung Zangbo River. This finding implies that stream order may be an appropriate clustering mode for AHG coefficients and exponents.

3.2.2 AMHG for all cross sections in the studied area

Section 3.2.1 determined that AMHG relationships exist in the same stream order of individual river basins but are not belong to a single river reach. This section will extend the range and further explore AMHG relations existing in the same stream order for all cross sections in the studied area (Fig. 4). Generally, the AMHG strength increases with increasing stream order and are mostly $R^2 > 0.6$ (excluding R^2 of order 8 streams) for cross sections located at order 7 and higher streams (Fig. 4). This result can be attributed to the variability of AHG exponents (*f* and *m*), which generally increase when the stream order increases from 5 to 8 (Fig. 5 e and f). However, the width exponents of order 9 streams plot within a relatively small range (0.032-0.192) compared to those of lower order streams (Fig. 5 d), which also result in an $R^2 > 0.6$.

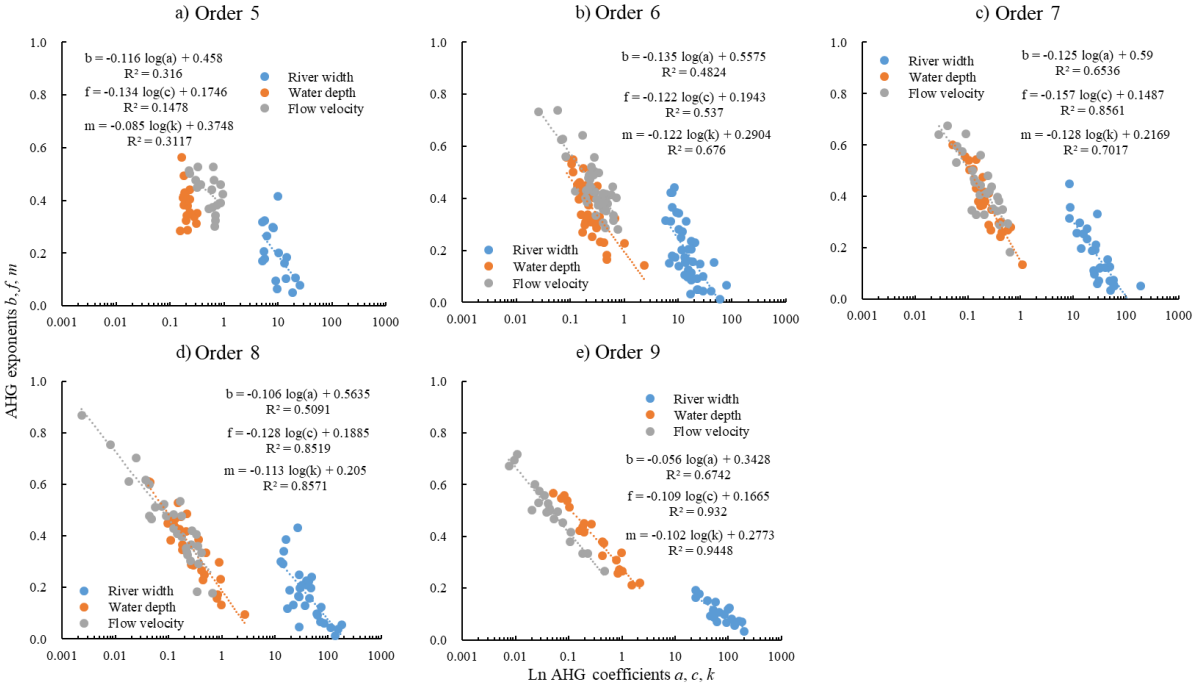

Figure 4 AMHG for all study cross sections located at different stream orders (5-9)

Similar to the AMHG relations of a given river reach (Fig. 2), the strength of the width-AMHG is generally weaker than the strengths of the depth- and velocity-AMHG relations. Compared with the AMHG strengths of the individual river basins (Fig. 3), the AMHG of all studied reaches generally shows equal or weaker strengths (Fig. 4 b-e), with a few exceptions (Figs. 3 a, c, g). Variability of the background environment within a basin is less than that of the whole studied region, which contribute to the increase in AMHG strength of the same river basin.

Relative relationships between the width-, depth-, and velocity-AMHGs change regularly with increasing stream order. Absolute values of AMHG slopes decrease with increasing stream order for all width, depth and velocity curves when the cross sections are located in the order 7-9 rivers (Fig. 4). This phenomenon can be used to explain the increase in congruent hydraulics with increased stream order (Table 2). Specifically, the depth-AMHG curve, which is located in the lower left direction relative to the velocity-AMHG curve, moves towards the upper right and finally plots to the upper right of the velocity-AMHG curve as the stream order increases from 5 to 9 (similarly, the velocity-AMHG curve moves towards the lower left direction with increasing stream order). Similar changes are found for the AMHG relations of individual river basins (Fig. 3). In addition, width-AMHG intercepts are larger than those of depth- and velocity-AMHGs for all stream orders (Fig. 4). Width-AMHG slopes of the order 5 and 6 streams are larger than those of velocity-AMHG slopes, but are smaller for the 7-9 order streams.

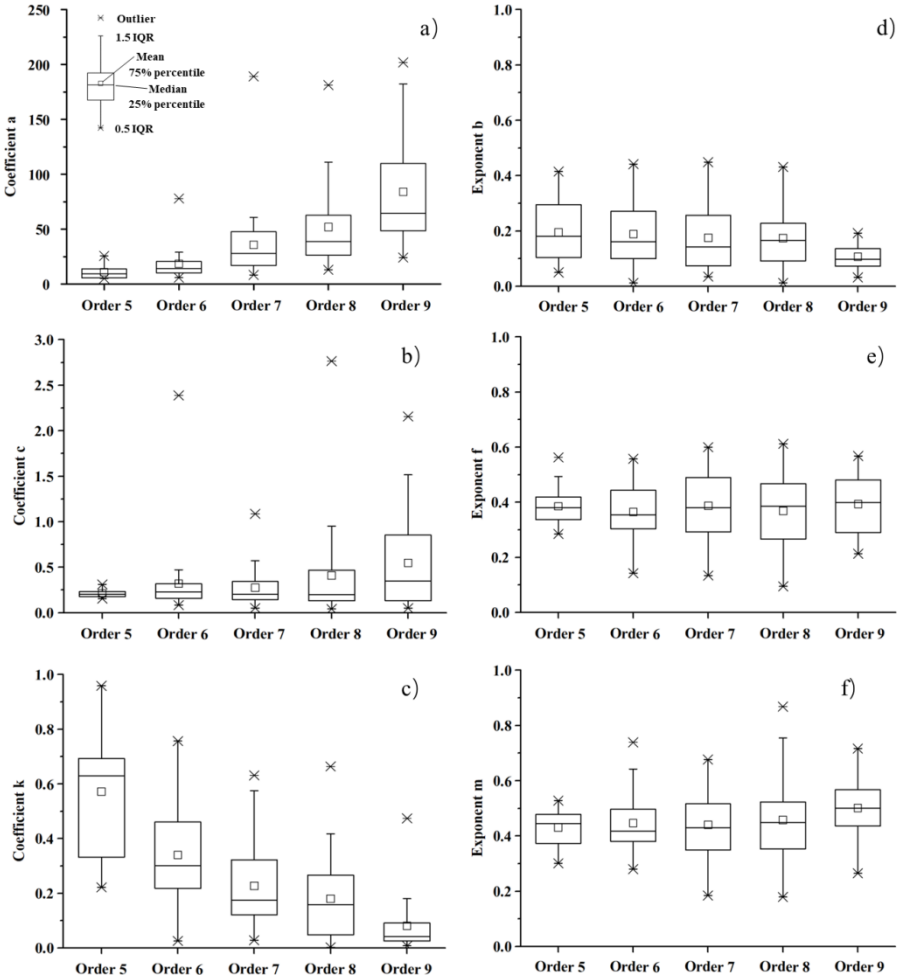

Figure 5 AHG coefficients (a-c) and exponents (d-f) for all cross sections of different stream orders

3.2.3 AMHG for cross sections located in transient regions or inside the QTP

For the cross sections that are located in different river reaches but in the same stream order, we further classified them into two types according to geomorphic units: cross sections inside the QTP and cross sections in transition regions (Table 3). We compared AMHG strengths in the same stream order for: 1) the whole studied region, 2) inside the QTP and 3) outside the QTP but in transient regions connecting the QTP and other geomorphic units (Table 3). Results indicate that AMHG strength overall increase after taking the geomorphic units into account. Compared with those generated by all cross sections, AMHG strengths generated by cross sections located in order 5, 6, 8 and 9 streams increase after taking the geomorphic units into account. For cross sections located in order 7 streams, no significant difference has been observed before and after taking the geomorphic units into account (total difference of AMHG strength (R^2) before and after taking the geomorphic units into account is -0.064). Overall, subdividing cross sections into two geomorphic units (inside the QTP or in transient regions) contributes to the increase of AMHG strength (Table 3).

3.3 Congruent hydraulics for AMHG and their geomorphic characteristics

3.3.1 Characteristics of congruent hydraulics

Stronger AMHG relationships contribute to improved estimations of congruent hydraulics (Gleason and Wang, 2015). AMHGs with an $R^2 > 0.5$ are used for the variation analysis discussed in this section (congruent hydraulics with no superscript [b] mark in Table 2). Generally, congruent discharges represented by width, depth and velocity (Q_{c_w}, Q_{c_d}, Q_{c_v}) show similar variation trends in different item groups (Table 2). The mainstreams of the Yellow River, the Jinsha River, the Yalong River, the Lantsang River and the Yarlung Zangbo River were successively distributed from north to south, excluding the Datong River (Fig. 1). Q_{c_w} shows an evident increasing trend from north to south, while Q_{c_d} and Q_{c_v} exhibit exceptions to this increase in the Yellow River and the Yarlung Zangbo River (Table 2). The Yarlung Zangbo River has the largest w_c, while the Lantsang River has the largest d_c and v_c.

Additionally, variations in w_c are smaller than those of d_c and v_c on a spatial scale. Excluding stream orders 5 and 6, all congruent hydraulics strictly increase with increasing stream order (Table 2).

Table 3 AMHG strengths of different stream orders and clustering modes

Stream order	Clustering modes	Strength (R^2)		
		Width-AMHG	Depth-AMHG	Velocity-AMHG
5	All cross sections	0.316	0.148	0.312
	Inside the QTP	0.540	0.431	0.406
	In transient regions	0.256	0.013	0.277
6	All cross sections	0.482	0.537	0.676
	Inside the QTP	0.348	0.705	0.618
	In transient regions	0.548	0.535	0.723
7	All cross sections	0.654	0.856	0.702
	Inside the QTP	0.492	0.811	0.409
	In transient regions	0.848	0.914	0.885
8	All cross sections	0.509	0.852	0.857
	Inside the QTP	0.511	0.894	0.822
	In transient regions	0.567	0.895	0.910
9	All cross sections	0.674	0.932	0.945
	Inside the QTP	0.694	0.976	0.924
	In transient regions	0.698	0.937	0.955

The percentage of rating curves intersecting within the observed discharge range can be used to predict the strength of AMHG (Gleason and Wang, 2015; Barber and Gleason, 2018). Among 96 congruent hydraulics (Table 2), 25% (24 out of 96 congruent hydraulics) are generated from weak AMHG strength items with $R^2 < 0.5$ (with superscript [b] mark), while 50% (48 out of 96 congruent hydraulics) are not within the observed discharge range. For those weak AMHG items, 79% (19 out of 24 congruent hydraulics, with superscript [c] mark in Table 2) are not within the observed discharge range. For those items with strong AMHG, only 40% (29 out of 72 congruent hydraulics) of them are not within the observed discharge range. These results indicate the consistency between the AMHG strength and the percentage of congruent hydraulics falling within the range of observed values for cross sections clustered by different items. Congruent hydraulics of the lower order streams (orders 5 and 6) and the higher order streams (order 9) often plot outside the observed range (Table 2 and Fig. 6). Most of the congruent hydraulics of cross sections located in stream orders 7-8 are within the observed range (Fig. 6).

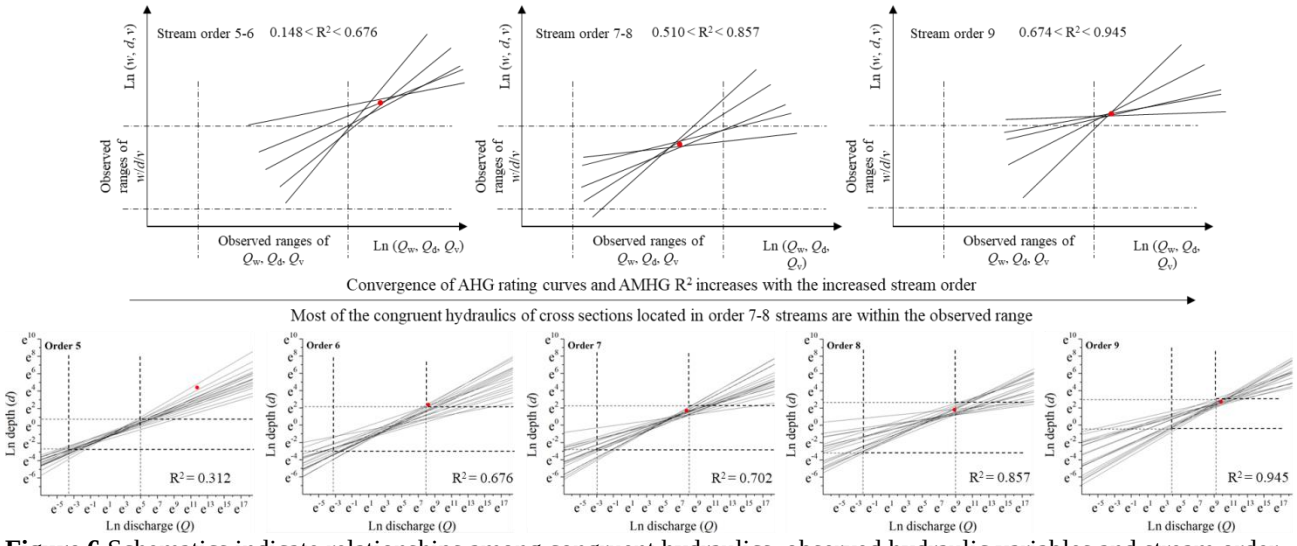

Figure 6 Schematics indicate relationships among congruent hydraulics, observed hydraulic variables and stream order (upper row); depth-AHG rating curves plotted in double logarithm coordinate systems for cross sections located in 5-9 stream orders (lower row). Red dots represent congruent hydraulics, area within dashed lines indicate the values of *w*/*d*/*v* and *Q* are within the in situ measured ranges.

3.3.2 Relationships between congruent hydraulics and observed hydraulics

To further study how the congruent hydraulics vary with observed hydraulics, the *congruent hydraulics* and corresponding in-situ measured *mean hydraulics* in Table 2 were plotted as linear functions with stream order (Fig. 7). Congruent *w* increases significantly with an increase in in-situ measured *w* when stream order increases. Though this exhibits an increasing trend, the increasing degrees for congruent *Q* and *d* are not as strong as that of the congruent *w* (Fig. 7). The above findings verifies the slight positive trend (R = 0.51) observed between mean *Q* and Q_c found by Barber and Gleason (2018), who determined that Q_c generally increases as the mean *Q* increases, though the mean *Q* cannot provide a reliable prediction of Q_c (R^2 = 0.26).

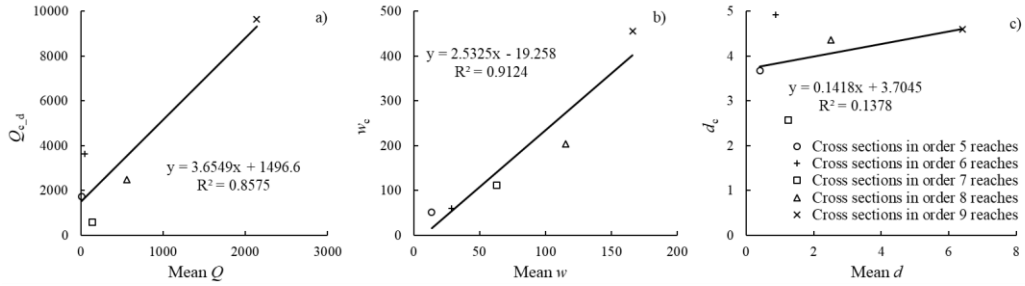

Figure 7 Congruent *Q*, *w*, *d* and in situ measured mean *Q*, *w*, *d* clustered by stream order

4 Discussions

4.1 Discussions on AMHG characteristics

Section 3.1 indicates an irregular array of AHG exponents and coefficients. Specifically, AHG exponents or coefficients along a river reach do not show a strict increasing or decreasing trend from upstream to downstream (Fig. 2 d and f). Set exponents *m* and coefficients *k* of the velocity-AHG as an example, *m* generally decrease with the increase of *k*. Based on this framework, however, increase of coefficients *k* and decrease of exponents *m* conform to the following sequence: DTR3, DTR5, DTR4, DTR1, DTR2 for the Datong River and LCR4, LCR3, LCR5, LCR2, LCR1 for the Lantsang River, respectively (Fig. 2 d and f). Not strict but an overall trends from downstream to upstream can be observed for the increase of coefficients *k* and decrease of exponents *f* along a river reach. Similar patterns can be found for coefficients (*a*, *c*) and exponents (*b*, *f*) of other river reaches (upper Yellow River and upper Jinsha River). Possible explanations might be: with the increased CA and the convergence of tributaries, *Q* increases downstream, which contributes to overall increasing trends of river width, water depth and flow velocity. Due to complex geology and geomorphology background for mountain rivers in the studied region, adjustments of *w*, *d* and *v* with *Q*, therefore, do not obey strict increasing law as the lowland rivers do, which leads to some irregularities of the distributions of the coefficients and exponents.

Combining Sections 3.2.1-3.2.3, AMHG does exist in cross sections of the same stream order; however, these cross sections do not belong to the same tributary or mainstream. The Jinsha, the Yalong, the Lantsang, the Nu and the Yarlung Zangbo River Basins exhibit narrow drainage basin shapes while the upper Yellow River Basin, located in northeast QTP, shows a relatively circular shape. Drainage basin shapes in the QTP and its boundary regions are largely controlled by geology and determined by geomorphology background. Large variations of the cross section morphologies in such complex region are expected, which might contribute to weak AMHG strengths. However, the results in Sections 3.2 provide evidence for AMHG as a widespread fluvial phenomenon in the same stream order. The existence of the AMHG that does not belong to a river reach indicates a hydraulic self-similarity of cross sections and a consistency of AHG coefficients and exponents that possibly exist in the same stream order. This consistency is not only shaped by flowing water but also possibly determined by the consistency of local climate, landscape, soil and vegetation. Cross channel AMHG reflects the consistency to a great extent. More tests should be conducted to see whether these AMHGs can exist in a wider geographical range and various climate types.

4.2 Factors affecting AMHG strength

AMHG strength generally increases with increasing stream order. Chi-square tests were used to verify the statistical significance of the increase in AMHG strength. In terms of the relationship between stream order and AMHG strength, the *P* values of the R^2 for river width, water depth and flow velocity using the chi-square test are 0.094, 0.069 and 0.014, respectively. The increasing trend of velocity-AMHG strength for stream order shows statistical significance with a *P* value < 0.05, while the other five increasing trends show no statistical significance ($P > 0.05$). Additionally, the width-AMHG strength shows a less significant increasing trend than those of the depth- and velocity-AMHG strengths.

Barber and Gleason (2018) indicated that the AMHG strength did not correlate to any available observed congruent hydraulics (Q, w, d and v) or the number of cross sections used to fit the AMHG relation. Stream order is not hydraulic parameters, but they are inherent attributes of a fluvial system and comprehensively synthesize characteristics of climate, landscape, soil and tectonic movement in the studied region. Several reasons contribute to the increase in AMHG strength with increased stream order:

1) Cross-section morphology is shaped by the geology, geomorphology, fluvial processes (water and sediment) and even tectonic movement present in the studied region. Lower-order streams (order 5 and 6 streams), representing an integrated record of past head cutting, bed incision and bank collapsing, have small CAs, which result in a small driving force and a large resistance. Discharges and stream power are small, while the boundary constraint is strong. The shaping power (river morphology and channel geometry that are shaped by flowing water and sediment) of the flowing water on the cross-section morphology is relatively small when compared to that of the higher order streams (order 7-9 streams). Geological control under a complex local landscape dominates the morphology of lower-order streams, which contributes to the high variability of cross-section morphology and less consistent variation in AHG coefficients and exponents. Outliers shown in Fig. 8 represent this inconsistency and are mainly located in lower order streams.

2) Higher-order streams have relatively large driving forces and small boundary constraints. Higher discharges and stream power indicate a greater contribution of contemporary fluvial processes to the shaping of cross-section morphology. This effect results in a relatively wide U-shaped cross section (Fig. 8; Fig. 5 a and d indicate an increase in coefficient a and a decrease in exponent b with increasing stream order, respectively). The wide U-shaped cross section corresponds to a flat channel bottom, steep banks and a relatively large shape exponent r in Dingman's cross-section geometry model (Dingman, 2007). In addition, the stream power increases along the river reach, which facilitates the regular changes in river width, water depth and flow velocity. As a result, AHG exponents vary consistently with the form of $b + f + m = 1$ in higher order streams (Fig. 8 b presents an inclined plane with some outlies located in order 5-7 streams).

In summary, the stability of cross sections increases with increasing stream order, which then contributes to the increase in AMHG strength. It can then be deduced that the AHG of cross sections located in the same stream order and shaped by discharges within similar ranges are dependent on each other but are not site specific, as previously theorized. These findings extend the AMHG theory and supports Rhodes' view (Rhodes 1977), who argued that "all cross sections of a given stream system are interrelated".

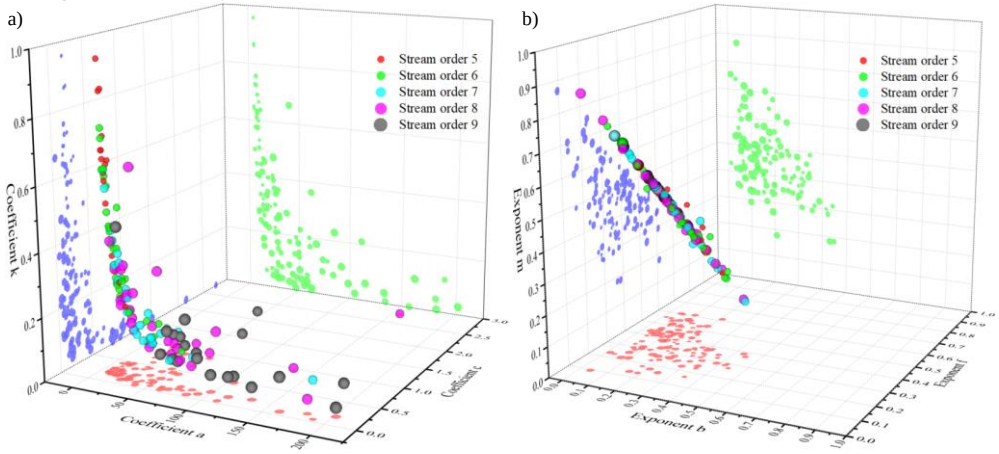

Figure 8 AHG coefficients (a) and exponents (b) for different stream orders in x-y-z coordinate systems (different sizes of shadows casted in x-y, x-z and y-z planes represent the values in different stream orders)

5 Summary and conclusions

Based on in-situ measurements of six major rivers and their tributaries originating from the QTP, this study first verified the existence of AMHG relations in the main streams of these rivers and then explored cross channel AMHG in the same stream order. Relationships among stream order and AMHG strength were studied. Congruent hydraulics and their relations to AMHG as well as in-situ measured hydraulics were tested. The following are the findings and implications of this research:

(1) AMHG exists in both main streams and cross sections located within the same stream order: a) Main streams of the Yellow River, the Datong River, the Yalong River, the Jinsha River, the Lantsang River and the Yarlung Zangbo River have at least one AMHG relation (width-, depth- or velocity-AMHG) with an $R^2 > 0.9$, which supports the

existence of AMHG in mountain rivers located in the southern and eastern portions of the QTP and demonstrates the power of using AMHG to predict AHG across the study river reaches. b) AMHG strength (R^2) increases with increasing stream order. The R^2 of cross sections located within order 7 and higher streams is largely > 0.6. c) Width-AMHG intercepts are larger than those of depth- and velocity-AMHGs for all stream orders. d) Congruent hydraulics generated from cross sections located in middle-scale rivers (order 7-8) are mostly within the observed range. The congruent *w* increases significantly with increasing in-situ measured *w,* while the increases of *Q* and *d* are relatively gradual as stream order increases.

(2) This study covers a large area of the eastern and southern portions of the QTP, including various environmental factors (such as climate, geology, landscape, vegetation, and soil) and stream patterns (single-thread rivers and multi-thread rivers). The findings from such complex areas indicate that AHG coefficients and exponents are functionally related and dependable between cross sections when they are in the same stream order. The cross channel AMHG is defined to reflect hydraulic self-similarity of cross sections and the consistency of AHG coefficients and exponents across reaches. The results of this research have the following implications: a) breaking the watershed divide boundary for AMHG; b) providing a basis for water and sediment simulation and research on river network structure and development; and c) providing the potential for using the AMHG theory for discharge estimation across the watershed divide, especially for data-scare mountain rivers.

(3) More testing is needed to verify the existence of AMHGs that are not located in a single river reach in complex climate, geologic and geomorphologic environments, especially for rivers in semi-arid and arid areas. The theoretical basis behind the mathematical artifact for AMHGs that existed in the same stream order should be studied further in the future.

Acknowledgements

This study was supported by the National Natural Science Foundation of China (Grant No. 51639005, 52009061, 52009062), Postdoctoral Innovation Talents Support Program of China (Grand No. BX20190177) and China Postdoctoral Science Foundation (2019M660656).

We appreciate the cooperation and efforts of all authors in producing the Proceedings. This will be a great symposium following the tradition of our sponsoring organizations.

References

Barber, C. A., Gleason, C. J. (2018). Verifying the prevalence, properties, and congruent hydraulics of at-many-stations hydraulic geometry (AMHG) for rivers in the continental United States. Journal of Hydrology 556, 625-633. https://doi.org/10.1016/j.jhydrol.2017.11.038

Bieger, K., Rathjens, H., Allen, P. M., Arnold, J. G. (2015). Development and evaluation of bankfull hydraulic geometry relationships for the physiographic regions of the United States. JAWRA Journal of the American Water Resources Association 51, 842-858. https://doi.org/10.1111/jawr.12282

Bonnema, M. G., Sikder, S., Hossain, F., Durand, M., Gleason, C. J., Bjerklie, D. M. (2016). Benchmarking wide swath altimetry-based river discharge estimation algorithms for the Ganges river system. Water Resources Research 52, 2439-2461. https://doi.org/10.1002/2015WR017296

Brinkerhoff, C. B., Gleason, C. J., Feng, D., Lin, P. 2020. Constraining remote river discharge estimation using reach-scale geomorphology. Water Resources Research 56, 1-24. https://doi.org/10.1029/2020WR027949

Brinkerhoff, C. B., Gleason, C. J., Ostendorf, D. W. (2019). Reconciling at-a-station and at-many-stations hydraulic geometry through river-wide geomorphology. Geophysical Research Letters 46, 9637-9647. https://doi.org/10.1029/2019GL084529

Ding, Y. J., Ye, B. S., Han, T. D., Shen, Y. P., Liu, S. Y. (2007). Regional difference of annual precipitation and discharge variation over west China during the last 50 years. Science in China Series D: Earth Sciences 50, 936-945. https://doi.org/10.1007/s11430-007-0042-8

Dingman, S. L. (2007). Analytical derivation of at-a-station hydraulic–geometry relations. Journal of Hydrology 334, 17-27. https://doi.org/10.1016/j.jhydrol.2006.09.021

Flores, J. A., Wu, J. Q., Stöckle, C. O., Ewing, R. P., Yang, X. (2020). Estimating river sediment discharge in the upper Mississippi River using Landsat imagery. Remote Sensing 12, 2370. https://doi.org/10.3390/rs12152370

Gleason, C. J. (2015). Hydraulic geometry of natural rivers: A review and future directions. Progress in Physical Geography: Earth and Environment 39, 337-360. https://doi.org/10.1177/0309133314567584

Gleason, C. J., Hamdan, A. N. (2017). Crossing the (watershed) divide: satellite data and the changing politics of international river basins. The Geographical Journal 183, 2-15. https://doi.org/10.1111/geoj.12155

Gleason, C. J., Smith, L. C. (2014). Toward global mapping of river discharge using satellite images and at-many-stations hydraulic geometry. Proceedings of the National Academy of Sciences 111, https://doi.org/4788-4791. 10.1073/pnas.1317606111

Gleason, C. J., Smith, L. C., Lee, J. (2014). Retrieval of river discharge solely from satellite imagery and at-many-stations hydraulic geometry: Sensitivity to river form and optimization parameters. Water Resources Research 50, 9604-9619. https://doi.org/10.1002/2014WR016109

Gleason, C. J., Wada, Y., Wang, J. (2018). A hybrid of optical remote sensing and hydrological modeling improves water balance estimation. Journal of Advances in Modeling Earth Systems 10, 2-17. https://doi.org/10.1002/2017MS000986

Gleason, C. J., Wang, J. (2015). Theoretical basis for at-many-stations hydraulic geometry. Geophysical Research Letters 42, 7107-7114. https://doi.org/10.1002/2015GL064935

Hagemann, M. W., Gleason, C. J., Durand, M. T. (2017). BAM: Bayesian AMHG-Manning inference of discharge using remotely sensed stream width, slope, and height. Water Resources Research 53, 9692-9707. https://doi.org/10.1002/2017WR021626

Hassan, M. A., Bird, S., Reid, D., Ferrer-Boix, C., Hogan, D., Brardinoni, F., Chartrand, S. (2019). Variable hillslope-channel coupling and channel characteristics of forested mountain streams in glaciated landscapes. Earth Surface Processes and Landforms 44, 736-751. https://doi.org/ 10.1002/esp.4527

Kebede, M. G., Wang, L., Li, X., Hu, Z. (2020). Remote sensing-based river discharge estimation for a small river flowing over the high mountain regions of the Tibetan Plateau. International Journal of Remote Sensing 41, 3322-3345. https://doi.org/10.1080/01431161.2019.1701213

Leopold, L. B., Maddock, T. (1953). The hydraulic geometry of stream channels and some physiographic implications. In "U.S Geological Survey Professional Paper 252", Washington D C.

Mark, D. M. (1984). Automated detection of drainage networks from digital elevation models. Cartographica 21, 168-178.

Martz, L. W., Garbrecht, J. (1992). Numerical definition of drainage network and subcatchment areas from Digital Elevation Models. Computers & Geosciences 18, 747-761.

Mengen, D., Ottinger, M., Leinenkugel, P., Ribbe, L. (2020). Modeling river discharge using automated river width measurements derived from Sentinel-1 time series. Remote Sensing 12, 3236. https://doi.org/10.3390/rs12193236

Ministry of Water Resources, P. R. China, (2016). Code for water flow measurement in open channels, GB 50179-2015. China Planning Press, Beijing, p. 202. (In Chinese).

Neal, J., Schumann, G., Bates, P. (2012). A subgrid channel model for simulating river hydraulics and floodplain inundation over large and data sparse areas. Water Resources Research 48, W11506. https://doi.org/10.1029/2012WR012514

Parker, G., Wilcock, P. R., Paola, C., Dietrich, W. E., Pitlick, J. (2007). Physical basis for quasi-universal relations describing bankfull hydraulic geometry of single-thread gravel bed rivers. Journal of Geophysical Research 112, F04005. https://doi.org/10.1029/2006JF000549

Parker, G., Wilkerson, G. V. (2011). Physical basis for quasi-universal relationships describing bankfull hydraulic geometry of sand-bed rivers. Journal of Hydraulic Engineering 137, 739-753. https://doi.org/10.1061/(ASCE)HY.1943-7900.0000352

Qin, C., Wu, B., Wang, Y., Fu, X., Xue, Y., Li, D., Li, M., Zhang, Y. (2020). Dynamic variability of at-a-station hydraulic-geometry for mountain rivers in the southeast Qinghai-Tibet Plateau: The cases of Yalong River and upper Jinsha River. Catena 194, 104723. https://doi.org/10.1016/j.catena.2020.104723

Rhodes, D. D. (1977). The b-f-m diagram: graphical representation and interpretation of at-a-station hydraulic geometry. American Journal of Science 277, 73-96. https://doi.org/10.2475/ajs.277.1.73

Rosenfeld, J. S., Post, J., Robins, G., Hatfield, T. (2007). Hydraulic geometry as a physical template for the river continuum: application to optimal flows and longitudinal trends in salmonid habitat. Canadian Journal of Fisheries and Aquatic Sciences 64, 755-767. https://doi.org/10.1139/f07-020

Shen, C., Wang, S., Liu, X. (2016). Geomorphological significance of at-many-stations hydraulic geometry. Geophysical Research Letters 43, 3762-3770. https://doi.org/10.1002/2016GL068364

Shields, F. D., Copeland, R. R., Klingeman, P. C., Doyle, M. W., Simon, A. (2003). Design for stream restoration. Journal of Hydraulic Engineering 129, 575-584. https://doi.org/ 10.1061/(ASCE)0733-9429(2003)129:8(575)

Singh, K. P., Broeren, S. M. (1989). Hydraulic geometry of streams and stream habitat assessment. Journal of Water Resources Planning and Management 115, 583-597. https://doi.org/10.1061/(ASCE)0733-9496(1989)115:5(583)

Song, X., Zhong, D., Wang, G., Li, X. 2020. Stochastic evolution of hydraulic geometry relations in the lower Yellow River of China under environmental uncertainties. International Journal of Sediment Research 35, 328-346. https://doi.org/10.1016/j.ijsrc.2020.02.003

Stall, J. B., Fok, Y. S. (1968). Hydraulic geometry of Illinois streams, WRC Research Report No. 15. Illinois State Water Survey, Urbanas Illinois. http://hdl.handle.net/2142/90172

Stall, J. B., Yang, C. T. (1970). Hydraulic geometry and low stream flow regimen, WRC Research Report No. 54. Illinois State Water Survey, Urbanas Illinois. https://www.isws.illinois.edu/pubdoc/CR/ISWSCR-131.pdf

Zhao, C. S., Pan, T. L., Xia, J., Yang, S. T., Zhao, J., Gan, X. J., Hou, L. P., Ding, S. Y. (2019). Streamflow calculation for medium-to-small rivers in data scarce inland areas. Science of The Total Environment 693, 133571. https://doi.org/10.1016/j.scitotenv.2019.07.377